J. Indian Chem. Soc.,
Vol. 96, May 2019, pp. 563-568

Hysteresis and energy storage properties study of $Ba_{0.5}Co_{0.5}Bi_2Nb_2O_9$ and $Ba_{0.5}Co_{0.5}Bi_2NbTaO_9$ nano ferroelectric ceramics prepared through chemical route: A comparative study

Mrinal K. Adak and Debasis Dhak*

Nanomaterials Research Lab, Department of Chemistry, Sidho-Kanho-Birsha University, Purulia-723 104, West Bengal, India

E-mail: debasisdhak@yahoo.co.in, debasis_dhak.chem@skbu.ac.in

Manuscript received online 04 December 2018, revised 13 March 2019, accepted 16 March 2019

$Ba_{0.5}Co_{0.5}Bi_2Nb_2O_9$ (BCoBN) and $Ba_{0.5}Co_{0.5}Bi_2NbTaO_9$ (BCoBNT) ferroelectric nano ceramics were prepared through chemical precursor solution decomposition method. P-E hysteresis study established that both the materials are non-linear ferroelectrics. The coercivity, remnant polarization and saturated polarization values were increased with increasing the applied electric field. BCoBNT showed the highest remnant polarization 3.96 $\mu C/cm^2$ at 40.24 kV/cm electric field with a high charge energy storage density of 220.76 J/cm^3. The highest energy efficiency was 84.74% found for BCoBN ceramics at 10.15 kV/cm applied electric field. BCoBNT showed the much higher polarization than BCoBN ceramics. The discharge and charge energy density were increased with increasing the electric field for both the ceramics. The energy efficiency value was regularly decreased for BCoBNT ceramics but some irregularity was found for BCoBN ceramics.

Keywords: Nanomaterials, ferroelectricity, FTIR, hysteresis, energy storage density.

Introduction

Pb-based ceramics are most important in electronic industries. It is their ferroelectric properties which make them so much demanding in electrical field from actuators to sensors and also they are found to be used as transducers[1,2]. But due to the presence of lead the ceramics are highly toxic which affect nature as well as human health. So, scientists have paid significant attention in the development of lead free piezeoelectric ceramics that will be environmental or eco-friendly with excellent properties. Aurivillius bismuth layered structured ferroelectrics (BLSFs) recently take much attention due to their high Curie temperature, high resistivity, ferroelectric random access memories (FRAMs), fatigue free properties, low aging rate[3,4]. As a result BLSFs are potentially used in fields of aerospace, aircraft, nuclear power and automotive industries[5]. The BLSFs have pseudo-perovskite structure with the general formula of $(A_{m-1}B_mO_{3m+1})^{2-}$ and $(Bi_2O_2)^{2+}$ layers along c-axis. Here 'A' is the monovalent, divalent or trivalent cations like Na^+, K^+, Sr^{2+}, Ca^{2+}, Ba^{2+}, Ln^{3+}, Bi^{3+} etc.; 'B' is the tetravalent, pentavalent or hexavalent cations like Fe^{3+}, Ti^{4+}, Zr^{4+}, Nb^{5+}, Ta^{5+}, Mo^{6+}, W^{6+} etc. in BO_6 octahedra and m indicates the number of BO_6 octahedra between $(Bi_2O_2)^{2+}$ layers[6,7]. The proper maintenance of the electrical response is the duty of $(Bi_2O_2)^{2+}$ layers. The layers behave as insulating as well as paraelectric at the same time[8]. $BaBi_2Nb_2O_9$ (BBN) is a leading one in the series of relaxor ferroelectric[9] where m = 2. The spontaneous polarization was observed for this material due to the displacement of the B-site cation and the tilting of the BO_6 octahedra.

The ferroelectric properties of BBN were greatly improved via the doping at 'A' and 'B' sites. Substitution at the Bi-site was also done by the researchers. Kannan *et al.* introduced Sm^{3+} at Bi^{3+} in $(Bi_2O_2)^{2+}$ layer that leads to the decrease of Curie temperature, dielectric constant, and dielectric loss with increasing Sm^{3+} content[10]. $(CaBi_2Nb_2O_9)_{1-x}(BaBi_2Nb_2O_9)_x$ ($0 \leq x \leq 1$) ceramics showed that the Curie point was decreased with increasing x and for $x \geq 0.8$ the ceramics showed a relaxor behavior[11]. Adamczyk *et al.* incorporated V^{5+} at Nb^{5+} site of BBN that improved the mechanical quality of the ceramics and a significant relaxor behavior of the ceramic was observed[12]. Substitution at 'A' site by Sr^{2+} gave typical relaxor behavior with strong dispersion of the complex relative dielectric permittivity[13]. Mohapatra *et al.* introduced Co^{2+}

in $Bi_2Fe_4O_9$ ceramics as $Bi_2Fe_{4(1-x)}Co_{4x}O_9$ ($0 \leq x \leq 0.02$) that exhibited non-Debye type relaxation and the remnant polarization was increased after the suitable amount of cobalt substitution[14]. Again the addition of 3 at% cobalt to $BiFeO_3$ film increased the remnant polarization from 49 to 72 $\mu C/cm^2$ observed by Naganuma *et al.*[15]. The partial substitution of Co^{2+} at Sr^{2+} of $SrBi_2Ta_2O_9$ enhanced the dielectric response[16].

In our previous study we substituted Co^{2+} at Ba^{2+} site of $BaBi_2Nb_2O_9$ as $Ba_{0.5}Co_{0.5}Bi_2Nb_2O_9$ (BCoBN)[17] and also Ta^{5+} at Nb^{5+} site as $Ba_{0.5}Co_{0.5}Bi_2NbTaO_9$ (BCoBNT)[18]. The materials showed good ferroelectric behavior with a significant non-Debye type relaxation. Here we discussed about the hysteresis and energy storage properties of BCoBN and BCoBNT ceramics.

Experimental

Chemical precursor solution decomposition method was used to synthesize the nanocrystalline BCoBN and BCoBNT ceramics. The detail of chemicals and synthesis procedure was reported in our previous publications[17,18].

The materials characterizations were done using X-ray diffraction study (XRD) (Philips, model: PW1710), Fourier transform infrared spectroscopy (FTIR) study (Perkin-Elmer spectrum two), thermo gravimetric analysis (TGA) (Perkin-Elmer STA 6000), Scanning electron microscope (SEM) (JEOL JSM5800) study. For the electrical characterizations the calcined powder was mixed with polyvinyl alcohol (PVA, 5 weight%) and pressed into a small pellet of 10 mm diameter with 1–2 mm thickness using a hydraulic press under an isostatic pressure of 0.05 MPa/cm^2. Here PVA acted as binding agent. The pellet was sintered at 750°C for 4 h in a muffle furnace. The both sides of the sintered pellets were electroded by the silver paste and dried at 200°C. The conductivity of the pellet surfaces were confirmed by a multimeter. The electroded pellet was used for P-E hysteresis study at room temperature using ferroelectric loop tracer (Merin India) at 50 kHz frequency.

Results and discussion

The XRD, SEM study of the BCoBN and BCoBNT ceramics were discussed in our previous publications[17,18]. The XRDs showed orthorhombic and tetragonal phase with space groups Cmc21 and I4/mmm for BCoBN[17] and BCoBNT[18] respectively. The lattice parameters were calculated to be *a* = 5.46 Å, *b* = 5.50 Å and *c* = 25.77 Å with unit cell volume 773.87 Å^3 for BCoBN while for BCoBNT the values were calculated to be *a* = *b* = 3.9394 Å, *c* = 24.4560 Å and unit cell volume = 397.05 Å^3. The powdered microstructure of BCoBN while observed through SEM showed an average grain size 168 nm with 62.9% polydispersity[17]. The average grain size of the sintered (950°C 4 h) pellets of BCoBNT exhibited through SEM showed 0.45 μm[18]. The chemical composition with stoichiometry was verified through energy dispersive X-ray (EDX) study of $Ba_{0.5}Co_{0.5}Bi_2Nb_2O_9$ and $Ba_{0.5}Co_{0.5}Bi_2NbTaO_9$ which satisfied the right composition of the two synthesized ceramics i.e. Ba, Co, Bi, Nb, and O for BCoBN and Ba, Co, Bi, Nb, Ta, and O for BCoBNT. No other impurity element was detected in EDX analyses.

The thermo gravimetric analysis (TGA) of the precursor mass of BCoBN and BCoBNT ceramics was done using a thermo gravimetric analyzer. The study was done in the heating rate of 5°C/min using nitrogen gas atmosphere from room temperature to 800°C. The percentage of weight loss with temperature was given in Fig. 1. A significant weight loss (>60%) was observed in the both cases. At the starting point a slow loss of water was observed after that a sharp change of the weight loss was observed at 500°C. This was due to the oxidation of the carbonaceous mass and decomposed of the metal complexes and TEA[19]. At this stage main reaction occured and evolution of various gases like water, CO, CO_2, NH_3 etc. was removed by the single step weight loss. No change of weight loss was observed above 650°C that indicated complete volatilization.

The FTIR spectrum of the calcined powder of BCoBN and BCoBNT was given in Fig. 2. The absorption bands at 3412 cm^{-1}, 1632 cm^{-1}, 841 cm^{-1} and 623 cm^{-1} were clearly observed for both the ceramics. The bands at 3412 cm^{-1} and 1632 cm^{-1} indicated O-H stretching and bending vibration modes of water molecules respectively. The presences of water molecules were due to the moisture in the sample or in sample compartment[20]. The peaks in the region between 1100–1200 cm^{-1} indicated the presence of O-O stretching frequency. The peaks at 841 cm^{-1} might be due to

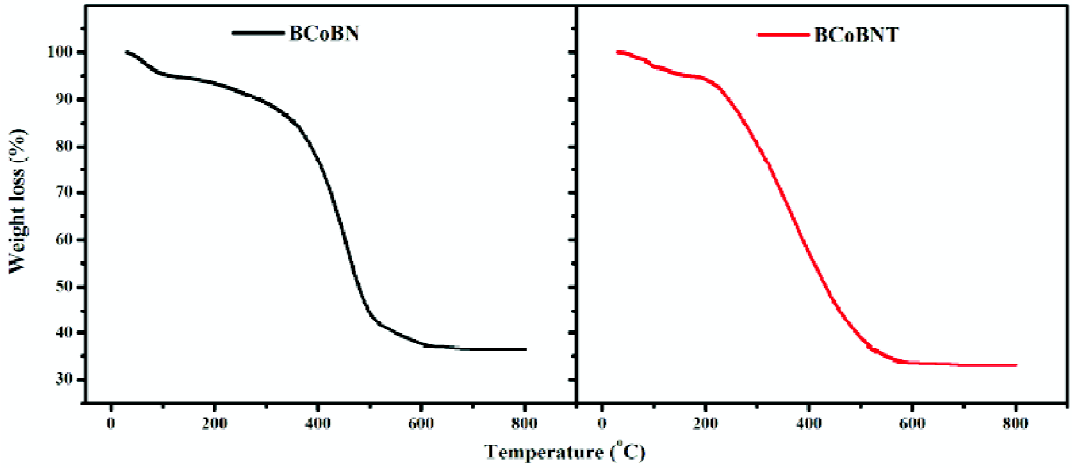

Fig. 1. Thermo gravimetric analysis of BCoBN and BCoBNT ceramics.

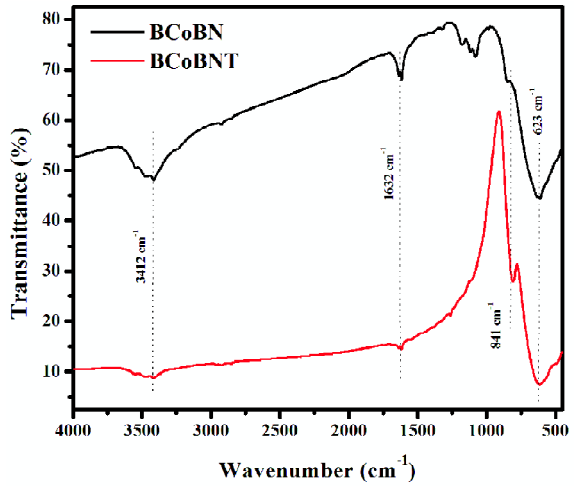

Fig. 2. Fourier transforms infrared spectroscopy study of BCoBN and BCoBNT performed at room temperature (25°C).

the Nb=O bond. Nakamoto *et al.* suggested band at 882, 871 cm^{-1} were for Nb=O bond[21]. Again a strong peak at 625 cm^{-1} indicated Nb-O bond in NbO_6 octahedra[20].

The ferroelectric P-E hysteresis study of BCoBN and BCoBNT was done at room temperature using 50 Hz frequency in the presence of different electric field. During the measurements the capacitor was fixed at 1 μF and resistor was fixed at 10 kΩ . The variation of the polarization with the increase of electric field of BCoBN and BCoBNT was given in Fig. 3(a) and 3(b). The coercivity (E_c), remnant polarization (P_r), saturated polarization (P_s) of both BCoBN and BCoBNT was given in Table 1. The table showed that BCoBNT exhibited high E_c, P_r, P_s than BCoBN ceramic which got increased with increasing applied electrical field. BCoBN

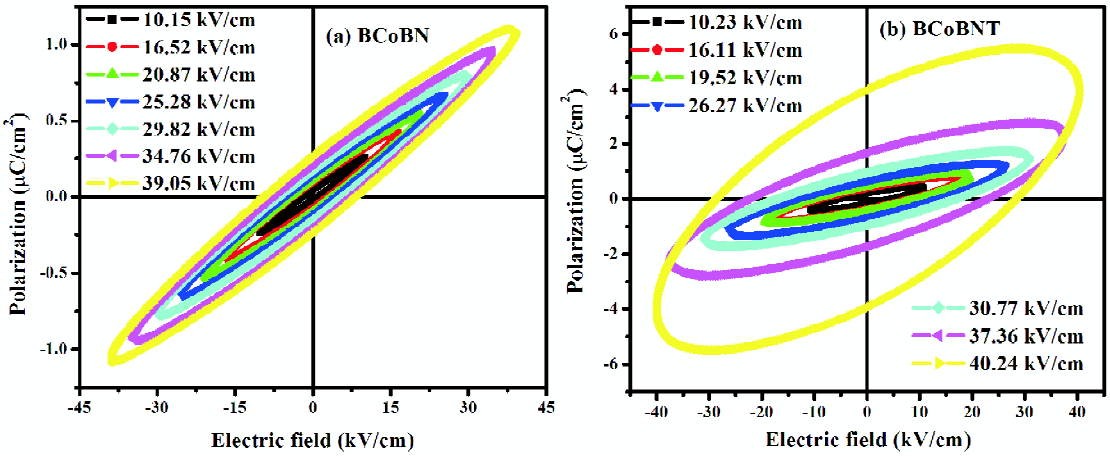

Fig. 3. P-E hysteresis study of (a) BCoBN and (b) BCoBNT ceramics from 10 kV/cm to 40 kV/cm electric field.

Table 1. Coercivity, remnance, saturated polarization value and energy storage properties of BCoBN and BCoBNT ceramics at different electric field

	Electric field (kV cm^{-1})	Saturated polarization (μC/cm^2)	Remnant polarization (μC/cm^2)	Coercivity (kV cm^{-1})	Discharge energy storage density (J cm^{-3})	Charge energy storage density (J cm^{-3})	η (%)
BCoBN	10.15	0.25	0.04	1.72	2.14	2.53	84.74
	16.52	0.42	0.08	3.36	5.58	6.99	79.91
	20.87	0.54	0.10	3.95	9.09	11.27	80.74
	25.28	0.66	0.14	5.19	13.37	16.81	79.55
	29.82	0.79	0.16	6.37	18.82	23.59	79.77
	34.76	0.95	0.21	7.49	25.86	33.09	78.15
	39.05	1.09	0.25	8.92	32.80	42.60	76.99
BCoBNT	10.23	0.44	0.21	5.34	2.33	4.46	52.29
	16.11	0.78	0.39	8.74	6.35	12.56	50.51
	19.52	0.89	0.46	10.03	8.60	17.51	49.16
	26.27	1.31	0.68	13.67	16.39	34.39	47.67
	30.77	1.73	0.96	16.97	23.66	53.11	44.55
	37.36	2.79	1.70	22.65	40.46	104.08	38.87
	40.24	5.49	3.96	28.49	61.41	220.76	27.82

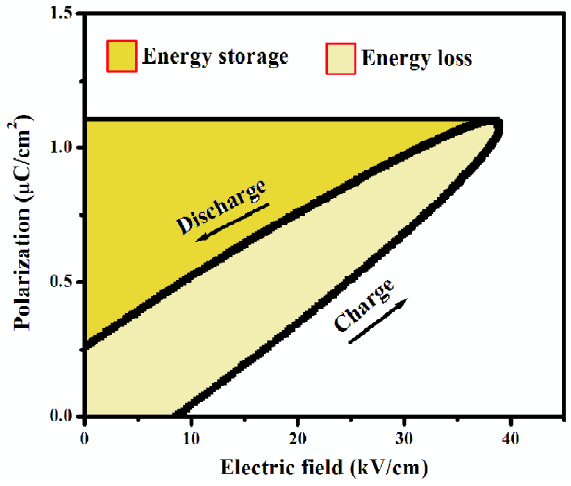

Fig. 4. Schematic diagram of energy storage and loss with the charge discharge cycle.

ceramic showed 0.25 μC/cm^2 remnant polarization at 29.05 kV/cm electrical field where as BCoBNT showed a high remnant polarization 3.96 μC/cm^2 at 40.24 kV/cm electric field.

The discharge energy density (*W*), charge energy density (*W′*), and energy efficiency (η) of BCoBN and BCoBNT were calculated from the P-E hysteresis data. The losses or unused energy density was expressed in Fig. 4 where the area was enclosed by charging and discharging curves. The discharge energy density (*W*) was calculated from the following equation[20]

$$W = \int_{P_r}^{P_m} EdP,\ 0 < E < E_{max} \quad (1)$$

Here P_m is the maximum polarization.

The charge energy density (*W′*) was calculated using the following equation

$$W' = \int_{0}^{P_m} EdP \quad (2)$$

and the energy efficiency

$$\eta = \frac{W}{W'} \quad (3)$$

The variation of the discharge energy density (*W*), charge energy density (*W′*) and energy efficiency (η) with the applied electric field for BCoBN and BCoBNT was given in Fig. 5. Table I showed that the energy efficiency gradually decreased for BCoBNT from 52.29 to 27.82% where as for BCoBN the change of energy efficiency was limited within a short range (84.74 to 76.99%). The lower value of η in BCoBNT indicated large hysteresis loses. If we compare BCoBN and BCoBNT on the basis storage application the former is more appropriate due to the low remnant polarization with slim hysteresis than later.

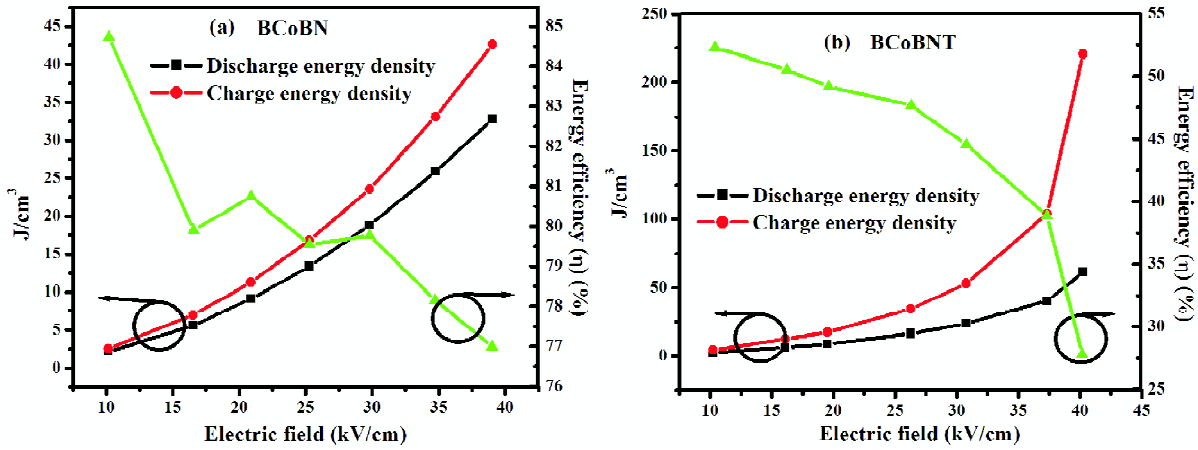

Fig. 5. Discharge energy density (*W*), charge energy density (*W'*) and percentage of storage efficiency (η) as a function of electric field for BCoBN and BCoBNT ceramics.

Conclusions

The nanocrystalline single phase BCoBN and BCoBNT ceramics were prepared using chemical precursor solution decomposition method. The TGA study confirmed the calcinations temperature 650°C. FTIR study showed the characteristics adsorption bands which were common for both the ceramics. The P-E study showed higher values of coercivity, remnant polarization and saturated polarization for BCoBNT than BCoBN ceramic. The lower value of remnant polarization of BCoBN demands better storage capacity than BCoBNT ceramics. A large hysteresis loss was observed for BCoBNT ceramics.

Acknowledgements

Author thanks SERB, DST, New Delhi, India for financial support (Grant No. SR/FT-CS-125, 2010). Author also thanks WB DST, Govt. of West Bengal, India (Grant No. 674(Sanc)/ST/P/S&T/15G/5/2016 dated 09/11/2016) for financial support. Mrinal K. Adak is thankful to the Council of Scientific and Industrial Research (CSIR), Government of India for the Senior Research Fellowship [File No. 09/1156(0004)/18-EMR-I].

References

1. M. Lal, M. Chandrasekhar, R. Rai and P. Kumar, *Am. J. Mater. Sci.*, 2017, **7**, 25.
2. R. Rai, S. Sharma and R. N. P. Choudhary, *Mater. Lett.*, 2005, **59**, 3921.
3. X. Xing, F. Cao, Z. Peng and Y. Xiang, *Ceram. Int.*, 2018, **44**, 17326.
4. Z. Peng, X. Zeng, F. Cao and X. Yang, *J. Alloys Compd.*, 2017, **695**, 626.
5. Z. Zhou, R. Liang, X. Shao, R. Huang, G. Cheng and X. Dong, *Ceram. Int.*, 2017, **43**, 11710.
6. E. Subbarao, *J. Phys. Chem. Solids*, 1962, **23**, 665.
7. R. E. Newnham, R. W. Wolfe and J. F. Dorrian, *Mater. Res. Bull.*, 1971, **6**, 1029.
8. S. K. Patri, P. L. Deepti, R. N. P. Choudhary and B. Behera, *J. Electroceramics*, 2018, 1.
9. D. Debasis, G. K. Tanmay and P. Panchanan, *Solid State Sci.*, 2007, **9**, 57.
10. B. R. Kannan and B. H. Venkataraman, *Ceram. Int.*, 2014, **40**, 16365.
11. H. Zhang, H. Yan and M. J. Reece, *J. Appl. Phys.*, 2010, **107**, 104111.
12. M. Adamczyk, L. Kozielski, M. Pawełczyk and M. Pilch, *Arch. Metall. Mater.*, 2011, **56**, 1163.
13. B. Behera, E. B. Araújo and A. F. Júnior, *Adv. Appl. Ceram.*, 2010, **109**, 1.
14. S. R. Mohapatra, B. Sahu, M. Chandrasekhar, P. Kumar, S. D. Kaushik, S. Rath and A. K. Singh, *Ceram. Int.*, 2016, **42**, 12352.
15. H. Naganuma, N. Shimura, J. Miura, H. Shima, S. Yasui, K. Nishida, T. Katoda, T. Iijima, H. Funakubo and S. Okamura, *J. Appl. Phys.*, 2008, **103**, 07E314.
16. C. Bedoya, C. Muller, F. Jacob, Y. Gagou, M. A. Fremy and E. Elkaim, *J. Phys. Condens. Matter.*, 2002, **14**, 11849.
17. M. K. Adak, S. S. Mondal, P. Dhak, S. Sen and D. Dhak, *J.*

Mater. Sci. Mater. Electron., 2017, **28**, 4676.

18. M. K. Adak, P. Dhak, A. Kundu and D. Dhak, *Adv. Mater. Lett*., 2016, **7**, 852.
19. D. Dhak, P. Dhak and P. Pramanik, *Appl. Surf. Sci*., 2008, **254**, 3078.
20. M. K. Adak, A. Mukherjee, A. Chowdhury, J. Khatun, U. K. Ghorai and D. Dhak, *J. Mater. Sci. Mater. Electron.*, 2018, **29**, 15847.
21. K. Nakamoto, "Infrared and Raman Spectra of Inorganic and Coordination Compounds", 6th ed., Wiley, 2009.